

## High Pressure Differential Thermal Analysis of *n*-Perfluoroalkanes

Shinsuke TSUBAKIHARA and Munehisa YASUNIWA

*Department of Applied Physics, Faculty of Science, Fukuoka University,  
Jonan-ku, Fukuoka 814-01, Japan*

(Received July 26, 1991)

**ABSTRACT:** Phase transitions of polytetrafluoroethylene (PTFE) oligomers (*n*-perfluoroalkanes),  $C_{20}F_{42}$ ,  $C_{24}F_{50}$ , and a polydispersed sample of *n*-perfluoroalkanes (molecular weight,  $MW = ca. 5000-20000$ ), denoted by L-PTFE, were studied at atmospheric pressure by differential scanning calorimetry and under high pressure up to 600 MPa by high pressure differential thermal analysis. Their phase diagrams were determined. The phase diagram of  $C_{20}F_{42}$  is quite different from that of PTFE. Below about 300 MPa, a sequence of crystal-crystal transitions denoted by Tr1 and Tr2 occurs in the isobaric heating process. In the pressure region between 300 and 400 MPa, there are two cases of crystal-crystal transitions, one case in which a pair of Tr3 and Tr4 occurs and the other case in which only Tr5 occurs. Above about 400 MPa, only Tr3 and Tr4 occur. The transition line of Tr4 has a terminal point at about 300 MPa. The phase diagram of  $C_{24}F_{50}$  is also similar to that of  $C_{20}F_{42}$ . On the other hand, the phase diagram of L-PTFE is different from these and identical to that of PTFE.

**KEY WORDS** *n*-Perfluoroalkane / Polytetrafluoroethylene / PTFE / Oligomer / *n*-Alkane / High Pressure / Phase Transition / Phase Diagram / Differential Thermal Analysis /

The phase transition of polytetrafluoroethylene (PTFE) was studied under high pressure, and its phase diagram shown in Figure 1 was determined.<sup>1,2</sup> At atmospheric pressure, two crystal-crystal transition points exist at 292 and 303 K. Clark and Muus<sup>3</sup> clarified by X-ray measurement that PTFE changes at 292 K from phase II (triclinic, 13/6 helix) to phase IV (hexagonal, 15/7 helix) and from phase IV to phase I (pseudohexagonal, irregular molecular conformation) at 303 K. The temperature range of phase IV decreases with pressure and disappears at about 200 MPa. Another solid phase (phase III) found by Bridgman<sup>4</sup> and Weir<sup>5</sup> appears above about 500 MPa. PTFE in phase III has an orthorhombic crystal structure and 2/1 helical conformation similar to those of polyethylene,<sup>6</sup> and higher density than that in phases I and II at the same pressure.<sup>2</sup>

Starkweather<sup>7</sup> carried out differential scanning calorimetry (DSC) of PTFE oligomers (*n*-perfluoroalkanes) and showed that  $C_{12}F_{26}$ ,  $C_{16}F_{34}$ ,  $C_{20}F_{42}$ , and  $C_{24}F_{50}$  have one or multiple crystal-crystal transition points in the low temperature range of 150—220 K.

Schwickert<sup>8</sup> reported that  $C_{20}F_{42}$  has two crystal-crystal transition points at 141 and 190 K at atmospheric pressure. He examined its crystal structures in all phases by X-ray measurement and obtained the following results.  $C_{20}F_{42}$  has a monoclinic crystal structure in two phases below 190 K and a rhombohedral one in the phase above the temperature. In the monoclinic phase between 141 and 190 K, molecular chains move longitudinally along the chain axes. On the one hand, they rotate around the chain axes in addition to the longitudinal motion in the rhombohedral one. Molecular conformation is

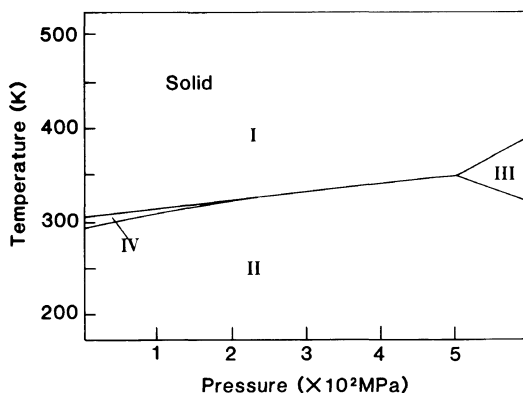


Figure 1. Phase diagram of PTFE.<sup>2</sup>

15/7 helix in all phases, irrespective of temperature.

The phase transitions of *n*-perfluoroalkanes under high pressure have not yet been studied and their phase diagrams are unknown. It is interesting to determine their phase diagrams and compare them with that of PTFE shown in Figure 1. In this work, high pressure differential thermal analysis (DTA) of *n*-perfluoroalkanes, *i.e.*, *n*-perfluoroeicosane ( $C_{20}F_{42}$ ), *n*-perfluorotetracosane ( $C_{24}F_{50}$ ), and a poly-dispersed sample of *n*-perfluoroalkanes (molecular weight,  $MW = ca. 5000-20000$ ), denoted by L-PTFE, was carried out up to 600 MPa to determine their phase diagrams. Change in the phase diagram of *n*-perfluoroalkane with molecular weight is discussed.

## EXPERIMENTAL

Samples  $C_{20}F_{42}$  and  $C_{24}F_{50}$  were purchased from Aldrich Chem. Co., Inc. (U.S.A.). The purity of  $C_{20}F_{42}$  was examined with gas chromatography using a flame ionization detector (FID) (Yanagimoto Shoji G2800-F). No impurity was detected in  $C_{20}F_{42}$ . L-PTFE ( $MW = ca. 5000-20000$ ), a polydispersed sample of *n*-perfluoroalkanes  $C_nF_{2n+2}$  ( $n = ca. 100-400$ ), was purchased from Wako Pure Chem. Industries, Ltd. The molecular weight of L-PTFE was determined from its melting

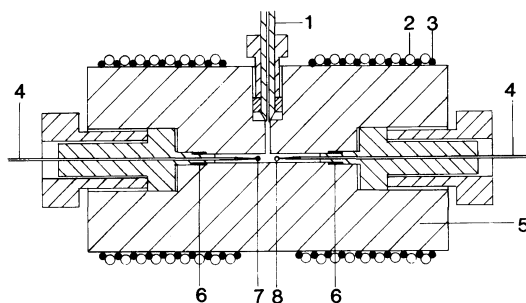


Figure 2. Schematic picture of a high pressure DTA apparatus. 1, high pressure pipe; 2, copper tube; 3, sheathed heater; 4, sheathed Alumel-Chromel thermocouple; 5, high pressure vessel; 6, copper seal; 7, sample; 8, reference.

point (579–595 K) based on Brady's equation,<sup>9</sup> *i.e.*,  $MW = 200/[685(1/T_m - 1/600)]$  where  $T_m$  is the melting point, used for determination of the number-average molecular weight of PTFE wax.

The phase transitions of *n*-perfluoroalkanes were examined at atmospheric pressure with a DSC apparatus (Rigaku Denki low temperature thermal analyzer). The samples were melt-crystallized at atmospheric pressure from original ones and put into aluminum containers. Their DSC curves in the heating process were obtained at a rate of  $5 \text{ K min}^{-1}$ .

High pressure DTA of  $C_{20}F_{42}$ ,  $C_{24}F_{50}$ , and L-PTFE was carried out up to about 600 MPa by an apparatus for high pressure, as shown in Figure 2. The apparatus made of beryllium copper containing 2% beryllium can withstand high pressure in a low temperature range below 200 K. As a pressure transmitting fluid, a low viscosity silicone oil (Shin-Etsu Chem. Co., KF-96L-1CS, 1cSt) was used. Hydrostatic pressure was detected within an accuracy of  $\pm 1 \text{ MPa}$  by a Bourdon's gauge (Heise Co., U.S.A.). The apparatus was cooled by circulating liquid nitrogen through the copper tube or spraying the low temperature gas of nitrogen on it, and heated at a constant rate using an automatic temperature controller. Samples melt-crystallized from original ones at atmospheric pressure were stuck on the

junction of an Alumel-Chromel thermocouple and covered by epoxy resin. Epoxy resin was also stuck on the junction of the other thermocouple and used as a reference material.

High pressure DTA was carried out in the isobaric heating process. At atmospheric pressure, the DTA apparatus was cooled to 20–30 K lower than the expected transition point at each measuring pressure. Pressure was then applied, and a DTA curve was obtained at a heating rate of  $5 \text{ K min}^{-1}$ .

## RESULTS AND DISCUSSION

Figure 3 shows the DSC heating curve of  $\text{C}_{20}\text{F}_{42}$ . It has three endothermic peaks at peak temperatures of 150, 201, and 437 K. Two peaks at 150 and 201 K are due to crystal–crystal transitions, and the highest temperature peak at 437 K is due to melting. The transition and melting points of the sample are very close to those reported by Starkweather.<sup>7</sup> On the other hand, the transition points are higher than those reported by Schwicker,<sup>8</sup> 141 and 190 K, respectively. Difference in purity between the two samples may cause differences in the transition points.

Figures 4a and b show the DTA heating curves of  $\text{C}_{20}\text{F}_{42}$  at various pressures. As will be shown later, the transition points obtained from the endothermic peaks formed five transition lines in the phase diagram determined from these DTA data. Therefore, the peaks in the figures were denoted by Tr1–Tr5 based on the transition lines to which their transition points belong. The endothermic peak of Tr1 at 0.1 MPa in Figure 4a is the same as the DSC transition peak at 201 K in Figure 3. The pressure change of the transition peak at 150 K could not be examined because the silicone oil used as the pressure transmitting fluid solidified at the low temperature. The DTA curve at 99 MPa has a new small endothermic peak of Tr2 on the slightly higher temperature side of the peak of Tr1. That is, crystal structure changes in two steps. The two

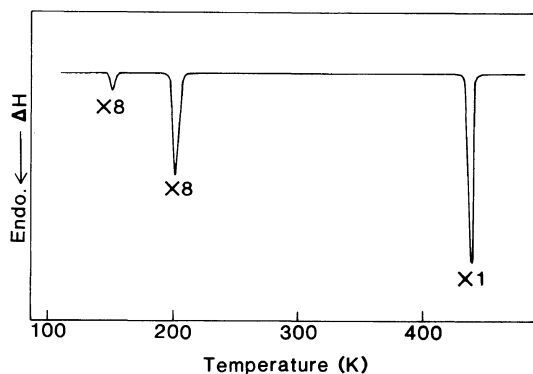


Figure 3. DSC curve of  $\text{C}_{20}\text{F}_{42}$  (heating rate,  $5 \text{ K min}^{-1}$ ). Each endothermic peak was magnified by the multiplicative number.

peaks of Tr1 and Tr2 were observed in the same way up to about 300 MPa, and their peak temperatures monotonically increased with pressure. These peaks, however, did not appear above about 300 MPa.

The DTA curve at 311 MPa has another endothermic peak of Tr5. The peak temperature of Tr5 also increased with pressure. On the one hand, that at 381 MPa (Figure 4b) has three endothermic peaks. The lowest temperature peak of Tr3 is a new peak different from those of Tr1, Tr2, and Tr5. The middle peak with small latent heat corresponds to Tr5. The highest temperature peak of Tr4 is also a new peak. In the pressure region between about 300 and 400 MPa, some kinds of DTA curves were observed even at the same pressure as will be shown later in detail. It is noted that each curve for this pressure region in the figures is merely one of them. Above about 400 MPa, only two endothermic peaks of Tr3 and Tr4 were observed. The peak temperatures of Tr3 and Tr4 increased with pressure, while their temperature difference of *ca.* 70 K did not vary with pressure.

The phase diagram of  $\text{C}_{20}\text{F}_{42}$ , determined by high pressure DTA, is shown in Figure 5. The marks ● and ■ represent crystal–crystal transition points and the mark ▲ represents melting points. These temperatures were

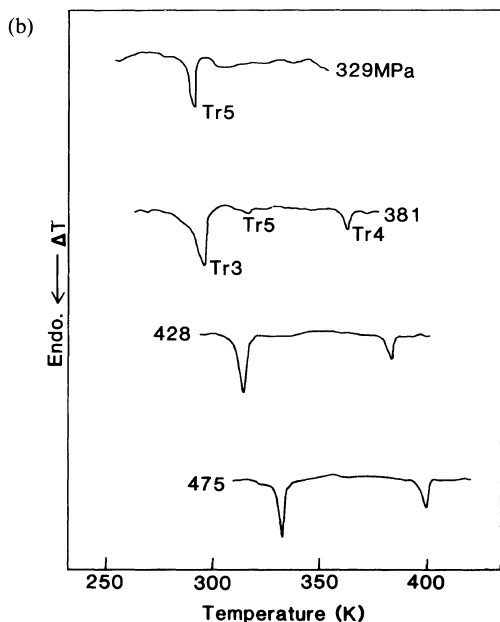
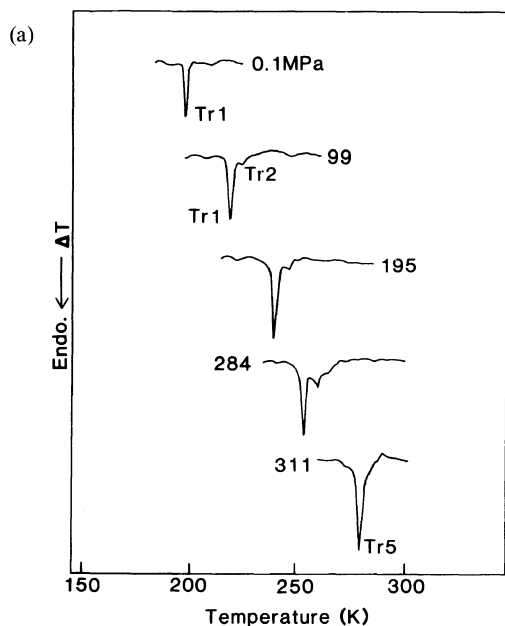


Figure 4. DTA curves of  $C_{20}F_{42}$  at various pressures (heating rate,  $5\text{ K min}^{-1}$ ).

obtained from the peak temperatures of DTA curves because they gave the most definitive temperatures. The mechanism of the crystal-crystal transition in the isobaric heating process

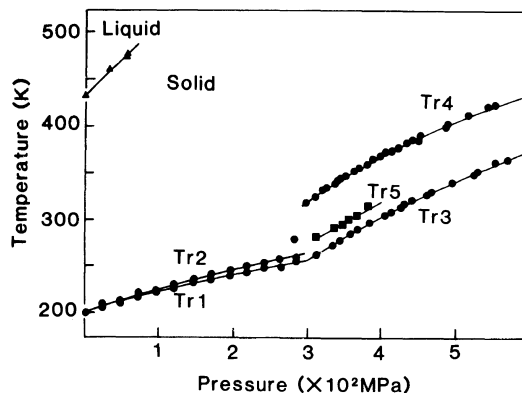


Figure 5. Phase diagram of  $C_{20}F_{42}$ : ● and ■, crystal-crystal transition points; ▲, melting points. These temperatures were obtained from the peak temperatures of DTA curves. In the pressure region between 300 and 400 MPa, there are two cases of crystal-crystal transitions in the heating process, one case in which a pair of Tr3 and Tr4 (●) occurs ( $\rightarrow\text{Tr3}\rightarrow\text{Tr4}\rightarrow$ ) and the other case in which only Tr5 (■) occurs ( $\rightarrow\text{Tr5}\rightarrow$ ).

considerably changes at about 300 MPa. Two crystal-crystal transitions Tr1 and Tr2 occur below about 300 MPa, while three other crystal-crystal transitions Tr3, Tr4, and Tr5 do above this pressure. The transition line of Tr4 has a terminal point at about 300 MPa.

Crystal-crystal transitions were reproducible except in the pressure region between 300 and 400 MPa. In this pressure region, there were two cases of crystal-crystal transitions in the heating process, one case in which a pair of Tr3 and Tr4 occurred ( $\rightarrow\text{Tr3}\rightarrow\text{Tr4}\rightarrow$ ) and the other case in which only Tr5 occurred ( $\rightarrow\text{Tr5}\rightarrow$ ). Both cases sometimes occurred together as shown by the DTA curve at 381 MPa in Figure 4b ( $\rightarrow\text{Tr3}\rightarrow\text{Tr5}\rightarrow\text{Tr4}\rightarrow$ ). Tr3 and Tr4 tended to be predominant compared to Tr5 at pressures near 400 MPa though Tr5 tended to be predominant compared to Tr3 and Tr4 at pressures near 300 MPa. The increase of the peak area at Tr3 and Tr4 caused the decrease of that at Tr5. There were also exceptional cases in which Tr3 and Tr4 with large peak area occurred at pressures near 300 MPa and in which Tr5 with large peak area did at pressures near 400 MPa.

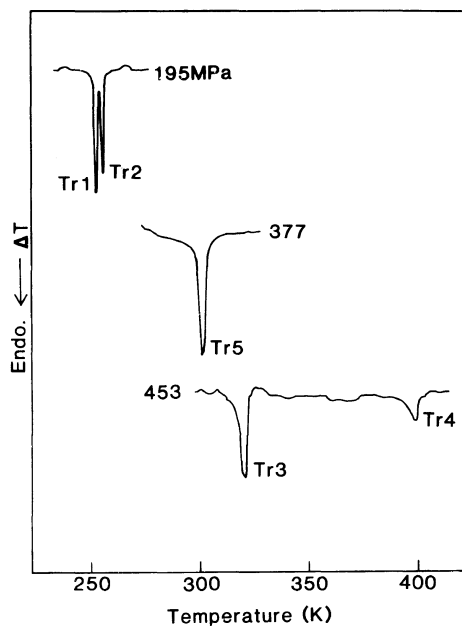


Figure 6. DTA curves of  $C_{24}F_{50}$  at various pressures (heating rate,  $5\text{ K min}^{-1}$ ).

Though they are not shown in Figure 4, their transition points are also included in the phase diagram.

Figure 6 shows the DTA heating curves of  $C_{24}F_{50}$  at various pressures. It was confirmed by DSC that  $C_{24}F_{50}$  had a sequence of crystal-crystal transition points, *i.e.*, 218 and 223 K at atmospheric pressure. The DTA curve at 195 MPa has the two endothermic peaks of these transitions denoted by Tr1 and Tr2. That at 377 MPa has another endothermic peak of Tr5, and that at 453 MPa has two other endothermic peaks of Tr3 and Tr4.

The phase diagram of  $C_{24}F_{50}$  is shown in Figure 7. It is similar to that of  $C_{20}F_{42}$  in Figure 5. In the case of  $C_{24}F_{50}$ , the mechanism of crystal-crystal transition in the isobaric heating process considerably changes in the pressure region between 300 and 400 MPa. This phase diagram, further, shows that two transition processes of  $\rightarrow\text{Tr3}\rightarrow\text{Tr4}\rightarrow$  and  $\rightarrow\text{Tr5}\rightarrow$  occur in the pressure region between about 350 and 390 MPa though the only single

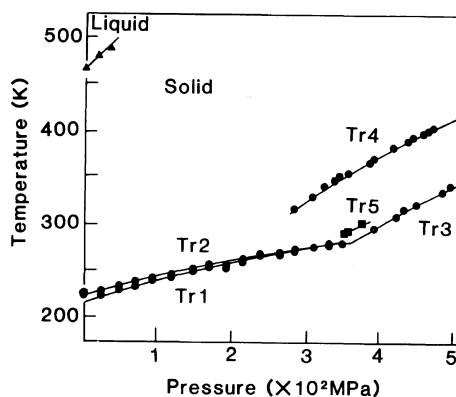


Figure 7. Phase diagram of  $C_{24}F_{50}$ : ● and ■, crystal-crystal transition points; ▲, melting points. These temperatures were obtained from the peak temperatures of DTA curves.

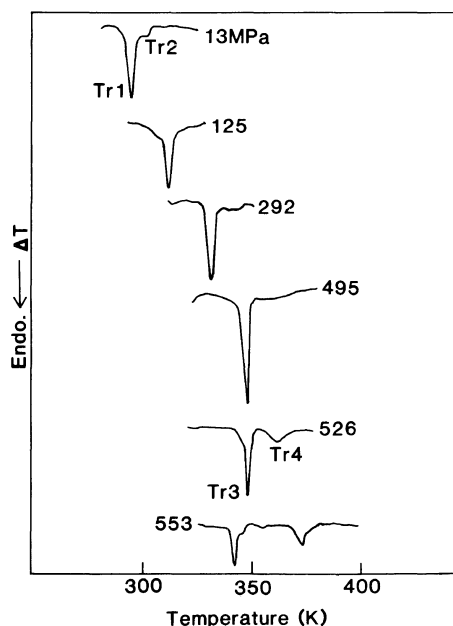
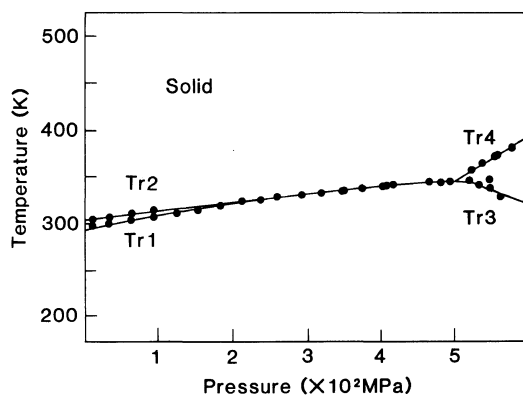


Figure 8. DTA curves of polydispersed L-PTFE ( $MW = \text{ca. } 5000\text{--}20000$ ) at various pressures (heating rate,  $5\text{ K min}^{-1}$ ).

peak showing  $\rightarrow\text{Tr5}\rightarrow$  was shown for 377 MPa in Figure 6.

Figure 8 shows the DTA heating curves of polydispersed L-PTFE. At atmospheric pressure, two crystal-crystal transition points exist at 292 and 303 K which are quite the same as



**Figure 9.** Phase diagram of L-PTFE: ●, crystal-crystal transition points. These temperatures were obtained from the peak temperatures of DTA curves.

those of PTFE. The two endothermic peaks of these transitions Tr1 and Tr2 combine at about 200 MPa, and a single peak appears up to about 500 MPa. Above about 500 MPa, two other endothermic peaks of Tr3 and Tr4 appear, and the temperature difference between them becomes wider with pressure. The phase diagram of L-PTFE is shown in Figure 9. The phase diagram is identical to that of PTFE (Figure 1). This indicates that the crystal structure and phase transition mechanism of L-PTFE are the same as those of PTFE.

In this work, it was clarified that the phase diagrams of C<sub>20</sub>F<sub>42</sub> and C<sub>24</sub>F<sub>50</sub> are quite different from that of PTFE, while that of L-PTFE is identical to it. Schwickert showed that the periodic layer structure of extended molecular chains exists in crystal of C<sub>20</sub>F<sub>42</sub>, and the molecular chain as a whole can move longitudinally and rotate around the chain axis as in the cases of *n*-alkanes.<sup>8,10</sup> There is not such periodic layer structure of molecular

chains in the crystal of L-PTFE because it has a wide distribution in chain length. It is also supposed that the longitudinal motion and rotation of a whole extended chain cannot take place due to the long length. These conditions of the layer structure and molecular motion of L-PTFE are the same as those of PTFE. Moreover, the phase diagrams of *n*-perfluoroalkanes are possibly determined by crystal structure and type of molecular motion. This may explain why the phase diagrams of C<sub>20</sub>F<sub>42</sub> and C<sub>24</sub>F<sub>50</sub> are different from those of L-PTFE and PTFE. To more definitively clarify the reason, it is desirable to study change in the phase diagram of *n*-perfluoroalkane with molecular weight using pure compounds between C<sub>24</sub>F<sub>50</sub> and PTFE, which do not include homologous impurities.

*Acknowledgment.* We thank Mr. Y. Mizoguchi and Mr. J. Ohishi for helping in the high pressure DTA work.

## REFERENCES

1. C. E. Weir, *J. Res. Natl. Bur. Stand.*, **50** 95 (1953).
2. S. Hirakawa and T. Takemura, *Jpn. J. Appl. Phys.*, **8**, 635 (1969).
3. E. S. Clark and L. T. Muus, *Z. Krist.*, **117**, 119 (1962).
4. P. W. Bridgman, *Proc. Am. Acad. Arts Sci.*, **76**, 55 (1948).
5. C. E. Weir, *J. Res. Natl. Bur. Stand.*, **46**, 207 (1951).
6. C. Nakafuku and T. Takemura, *Jpn. J. Appl. Phys.*, **14**, 599 (1975).
7. H. W. Starkweather, Jr., *Macromolecules*, **19**, 1131 (1986).
8. H. Schwickert, Doctoral thesis, Universität Mainz, 1984.
9. J. D. Brady, U. S. Patent 3 067 262 (Dec. 4, 1962).
10. G. R. Strobl, *J. Polym. Sci., Polym. Symp. Ed.*, **59**, 121 (1977).